POLITECNICO DI TORINO
Repository ISTITUZIONALE

ReGrid: A Highly Conformable and Ultrasound Transparent Patch for HD-sEMG Detection

Original
ReGrid: A Highly Conformable and Ultrasound Transparent Patch for HD-sEMG Detection / Cerone, G.L., Vieira, T., Gazzoni, M., Botter, A.. - In: IEEE TRANSACTIONS ON NEURAL SYSTEMS AND REHABILITATION ENGINEERING. - ISSN 1534-4320. - 34:(2026), pp. 1048-1059. [10.1109/tnsre.2026.3663330]

Availability:
This version is available at: 11583/3010594 since: 2026-05-06T10:42:55Z

Publisher:
IEEE

Published
DOI:10.1109/tnsre.2026.3663330

Terms of use:

This article is made available under terms and conditions as specified in the corresponding bibliographic description in the repository

Publisher copyright

(Article begins on next page)

12 October 2026

ReGrid: A Highly Conformable and Ultrasound Transparent Patch for HD-sEMG Detection

Giacinto L. Cerone, *Member, IEEE*, Taian Vieira, Marco Gazzoni, and Alberto Botter, *Member, IEEE*

***Abstract*— This study describes a novel high-density EMG dry electrode grid (ReGrid) based on a thin-film patch highly conformable to the skin and fully ultrasound-transparent. ReGrid consists of a 15 μm-thick polyurethane membrane housing silver electrodes and traces inkjet-printed on the skin-facing side. A waterproof medical-grade adhesive layer protects the outer surface, while a flexible PCB connector ensures the connection with the acquisition system. Bench tests were conducted to assess mechanical conformability and US transparency. Results showed that ReGrid conformed to curved surfaces, other than allowing for B-mode US imaging without artifacts: both the support and the electrodes resulted transparent to ultrasound. In-vivo tests on the tibialis anterior muscle confirmed low and stable electrode-skin impedance and noise levels comparable to conventional gel-based electrodes. HD-sEMG signals were recorded during isometric contractions at two force levels (10% and 20% MVC), with and without a US probe placed directly over the electrodes. Conduction velocity estimates and HD-sEMG decomposition outcomes were not significantly affected by the US probe, nor was the level of power-line interference. Thanks to its conformability, ultrasound transparency, and high signal quality, ReGrid enables combined HD-sEMG and ultrasound acquisitions from the same muscle region, supporting novel applications such as 3-D and panoramic ultrasound imaging integrated with HD-sEMG.**

***Index Terms*— Electromyography, high-density EMG, tattoo electrodes, motor unit decomposition, ultrasound transparent electrode.**

I. Introduction

OVER the past two decades, high-density surface electromyography (HD-sEMG) has gained considerable attention in different fields, ranging from basic neurophysiology, to sport, and ergonomics [1], [2], [3], [4]. HD-sEMG employs arrays of closely spaced electrodes to provide a two-dimensional representation of the electric potentials generated by the underlying muscle. This spatial mapping of muscle excitation provides a deeper understanding of both peripheral and central properties of the neuromuscular system than the localized detection offered by traditional bipolar recordings [5], [6], [7]. The detection of HD-sEMG has traditionally faced two main technological challenges. The first is the encumbrance of the biopotential acquisition systems, which has often restricted the use of HD-sEMG to laboratory settings. Recent advancements in the design and development of biopotential acquisition systems [8], [9] contributed to overcome this limitation by simplifying experimental setups and improving the usability of HD-sEMG in increasingly demanding experimental conditions [8]. The second is related to the detection systems (i.e. system of electrodes) and in particular to: i) the need for small electrodes, a few millimeters in diameter, which leads to high electrode-skin impedance with negative effects on signal quality [10], [11], [12], and ii) the need to obtain a good adhesion of the whole electrode grid to the skin, even on highly curved surfaces [12], [13], [14]. The current HD-sEMG electrode grid technology, which has remained largely unchanged over the past twenty years [5], does not provide a comprehensive solution to both issues. It is based on flexible Printed Circuit Boards (PCB) housing a grid of silver pads (the electrodes) and the conductive tracks connecting them to an external connector. The flexible printed circuit is attached to the skin through a die-cut bi-adhesive pad, with holes in correspondence of the electrodes. The electrode-skin contact is established by filling the foam cavities with conductive gel or paste. This state-of-the-art technology provides a mechanically stable and low-impedance contact interface between skin and electrodes, allowing, in combination with the acquisition system, to collect high-quality EMGs [12]. However, it presents some technological bottlenecks currently limiting its applicability to a wider range of experimental contexts. From the mechanical point of view, the structure composed of a flexible PCB with the underlying adhesive pad limits the capability of the grids to conform to anatomical regions characterized by curved surfaces. Moreover, an important practical aspect is that grid preparation requires time and, albeit minimal, operator expertise to ensure proper alignment between the foam cavities and the electrodes, as well as dosing the correct amount of conductive gel or paste filling the cavities [15]. Other limitations are application

Received 23 June 2025; revised 11 January 2026; accepted 7 February 2026. Date of publication 10 February 2026; date of current version 19 February 2026. *(Corresponding author: Giacinto L. Cerone.)*

Giacinto L. Cerone and Alberto Botter are with the Laboratory for Engineering of the Neuromuscular System (LISiN), Department of Electronics and Telecommunications, PoliToBIOMed Laboratory, Politecnico di Torino, 10129 Turin, Italy, and also with ReC Bioengineering Laboratories S.r.l., 10129 Turin, Italy (e-mail: giacintoluigi.cerone@polito.it).

Taian Vieira and Marco Gazzoni are with the Laboratory for Engineering of the Neuromuscular System (LISiN), the Department of Electronics and Telecommunications, and the PoliToBIOMed Laboratory, Politecnico di Torino, 10129 Turin, Italy.

This article has supplementary downloadable material available at https://doi.org/10.1109/TNSRE.2026.3663330, provided by the authors.

Digital Object Identifier 10.1109/TNSRE.2026.3663330

© 2026 The Authors. This work is licensed under a Creative Commons Attribution-NonCommercial-NoDerivatives 4.0 License.
For more information, see https://creativecommons.org/licenses/by-nc-nd/4.0/

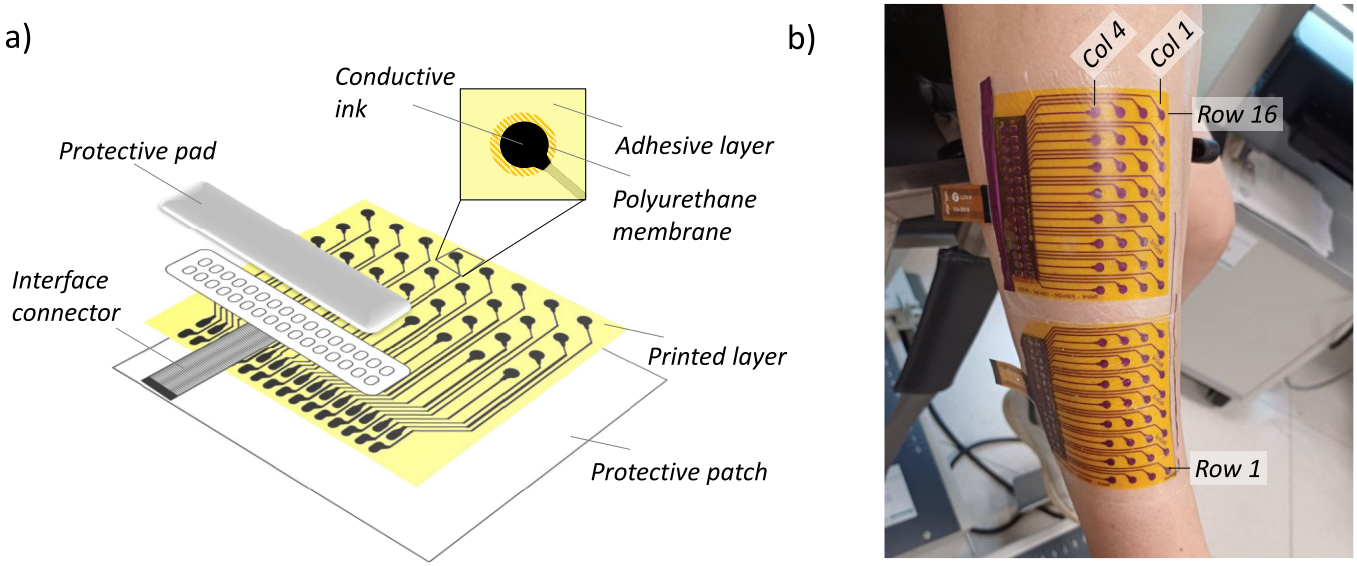

Fig. 1. a) Grid structure. ReGrid is a dry-electrode patch composed of: (i) a Polyurethane (15 μm thick) membrane housing (ii) inkjet-printed silver electrodes, traces and connection pads, (iii) a waterproof, medical-grade, adhesive patch acting as protective layer; iv) a flexible PCB (0.8 mm thick polyimide) interfacing the detection and acquisition systems. b) A picture of two ReGrids positioned on the tibialis anterior muscle.

specific. For instance, it is worth mentioning the growing interest in integrating ultrasound imaging with HD-sEMG, as this combination provide complementary information, opening new research possibilities for the study of electrical and mechanical muscle properties [16], [17], [18], [19], [20], [21]. Current HD-sEMG grid technology does not allow the simultaneous acquisition of sEMG and ultrasound images from the same muscle region, as the acoustic impedance of the flexible printed circuits and the presence of air gaps in the bi-adhesive foam lead to shadow-like artifacts hindering the ultrasound imaging through the grid (cf. Fig. 1 in [22]).

In the last decade, technological solutions have been proposed to design simpler, more reliable, and more flexible grids of electrodes. In response to the need for enhanced skin conformability and improved ease of use, dry electrode grids have emerged. These electrodes are designed to adhere directly to the skin without requiring adhesive layers or conductive media on the electrode surface [14], [23], [24], [25]. More recently, a new research direction has explored the use of thin-film patches [26], [27], [28], [29], [30], [31] and tattoo-based approaches [32], [33], [34]. Although promising, these solutions still present challenges related to the manufacturing process, (often requiring costly and complex fabrication processes) and reliability issues related to the electrical stability of traces and electrode-amplifier connections [34]. In particular, a critical issue remains the connection to the amplification system, as the interface between the highly flexible tattoo or thin-film supports and the rigid connector elements creates an intrinsic point of fragility. This limitation undermines the advantages of using highly flexible and conformable materials, as the connection system remains bulky, unstable, and difficult to reproduce. Furthermore, traces connecting electrodes to the amplifier system are often printed on the layer in contact with the skin and cannot be insulated without creating air gaps, leading to an increase of contact area, contact instability, and possible EMG-crosstalk coming from the coupling between the traces and the skin [22], [34]. These observations are evidenced by the limited number of scientific studies employing these electrodes in experimental studies, even in controlled laboratory settings.

From the perspective of ultrasound transparency requirement, standard grids based on textile or PCB supports and metal electrodes do not allow ultrasound imaging through them, creating long shadow-like artifacts on the echographic image due to the iper-echogenic nature of such materials [22]. Alternative materials such as hydrogel [35], thin films or tattoo-like [34] solutions coupled with thin-wire or conductive-ink electrodes exhibit an acoustic impedance compatible with ultrasound transparency over the entire electrode surface. This property has been exploited to develop large, bipolar electrodes suitable for combined EMG and ultrasound detections [35], [36], [37]. Another key feature for enabling the possibility of concurrently acquire HD-sEMG signals and US images is the electrodes grid waterproofness to limit the short circuits mediated by the US gel.

In this study, we describe the design and characterization of a new grid of electrodes that contends with issues of growing interest in EMG studies: conformability to the skin and complete transparency (both on electrodes and traces) to ultrasound. More specifically, we designed and developed a new electrode-grid technology based on thin-film patch allowing to: i) conform to surfaces and body locations characterized by sharp and non-uniform curvatures; ii) guarantee stable and adhesive electrode-skin contact, also in presence of dry electrodes; iii) concurrently acquire US images and HD-sEMG signals from the same muscle region.

II. Methods

A. Electrode Grid Design

ReGrid (Fig. 1) is a dry-electrode patch composed by four main elements: i) a Polyurethane (PU - 15 μm thickness) membrane; ii) conductive elements (silver electrodes, traces

and connection pads) deposited on the skin-facing side of the PU membrane through inkjet printing; iii) a water-proof, medical-grade, adhesive patch overlying the outer side of the PU membrane, which provides mechanical support and protects the grid from external agents such as water and ultrasound gel; iv) a flexible PCB (interface connector) that ensures electrical continuity between the printed connection pads and the biopotential amplifier.

The conductive elements are deposited onto the PU membrane using a standard inkjet printer (Epson EcoTank ET-2810, Suwa, Japan) loaded with a silver nanoparticle-based conductive ink (Metalon ® JS-ADEV ET010, NovaCentrix, Austin (TX), USA). The choice of using a PU membrane as a support layer for the printed elements is due to its US-transparency and compatibility with ink-jet printing technology. However, being the PU thickness (80 μm) below the minimum thickness accepted by standard inkjet printers, a water-soluble paper sheet was coupled to the PU film and used as a sacrificial coupling material during printing.

Electrodes (2 mm radius) were arranged in an eight-by-four grid with 10 mm Inter-Electrode Distance (IED), to reproduce arrangements often used in HD-sEMG studies. Traces (0.1 mm thick) were designed to connect electrodes to the connection pads serving as interface to flexible PCB connector (interface connector in Fig. 1a). The printed sheet (PU membrane coupled with the water-soluble paper) is baked at 150 °C for 15 minutes as suggested by the conductive ink manufacturer (NovaCentrix, Austin (TX), USA). After baking, the PU membrane is separated from the water-soluble paper by means of pure water. Afterwards, a medical-grade adhesive and water-proof protective patch (Hydrofilm, Heidenheim an der Brenz, Germany) is attached to the external side of the PU membrane. Conductive traces on the skin side are protected by means of a 70 μm thick medical-grade adhesive glue (3M^{TM} Medical Transfer Adhesive 4075, 3M, Saint Paul, Minnesota, USA). The interface connector consists of a flexible PCB (0.8 mm thick polyimide) and is connected to the terminal pads of the grids using a silver-loaded adhesive (MP011123, Multicomp Pro, London, United Kingdom), as described in Cerone et al. 2021 [14].

B. Experimental Validation

The following sections outline the experimental protocols carried-out to characterize the ReGrid electrode system in terms of i) mechanical and electrical properties, ii) quality of detected HD-sEMG signals, and iii) performance in simultaneous acquisitions of HD-sEMG and US from the same muscle region. The validation tests were categorized into bench and in-vivo experimental protocols. In-vivo measurements were conducted in accordance with the Declaration of Helsinki and the procedure approved by the Regional Ethics Committee (ASL 1 Torino, Italy, approval n. 0010610). Informed consent was obtained from participant after receiving detailed explanation of the study procedures.

1) Bench Test: Conformability: Grid conformability is a crucial feature influencing both the performance and the usability of a HD-sEMG detection system. Conformability is defined as the ability of the electrode system to conform to the underlying surface while maintaining the integrity of the electrode-skin interface. For electrode grids, conformability assessment is generally based on qualitative and semi-qualitative tests, which often lack standardized and objective metrics. Typically, conformability is assessed either by evaluating the electrical conductivity of an electrode grid when applied to elastic objects with varying shapes [38], or through visual inspection of its adhesion to curved surfaces or specific body regions. The first approach is valid for characterizing grid elasticity, while the second is mainly used as a proof-of-concept but lacks objective, reproducibile metrics. Based on these observations, a new bench-based approach for characterizing electrode grids conformability has been proposed. Grid conformability has been evaluated by applying the grid on a 3D-printed semi-spheric solid whose surface was made electrically conductive through spray coating paint (Grafite 200 ML spray, 1281411 Dewpro Engineering. RSA), so that all the electrodes are theoretically short circuited. Grid conformability was evaluated by counting the number of electrodes showing a missing contact with the underlying conductive surface, assessed using a digital multimeter configured as lead tester (Fluke 179, Fluke Corporation, Everett, Washington, US). The test was carried-out on two 64-electrode grids (8 × 8, 10 mm IED, 50 cm^2 surface): one ReGrid patch and one state-of-the-art HD-sEMG grid composed of a flexible polyimide circuit (254 μm thick) with a 2-mm thick bi-adhesive foam. Each 64-electrode grid was obtained by placing two adjacent 32-channel grids of the same type used in the in-vivo experiments. The test was repeated using three different curvature radii of the semi-spheric support (41 mm, 57 mm, 78 mm). Curvature radii have been selected to mimic the median curvature radius of three body regions (chin, knee and shoulder) [39] selected as representative worst-case conditions both in terms of curvature radius and surface geometry.

2) Bench Test: Transparency to Ultrasound: A general-purpose US phantom (model 054GS, CIRS, Norfolk, Virginia, USA) was used to assess the transparency of ReGrid to ultrasound. Ultrasound images were detected using a portable US device (ArtUs, Telemed, Lithuania - equipped with a 12MHz linear probe) in two conditions: with and without the presence of ReGrid between the probe and the phantom. The same hyperechogenic markers were imaged in both conditions while keeping the ultrasound device settings unchanged. The position of the probe was marked on the phantom surface to ensure the same scanning area for both experimental conditions. Contrast-to-noise ratio (CNR) was calculated and used as an image quality index [37]:

$$CNR = 20\ log_{10}\left(\frac{|\mu_{test} - \mu_{bck}|}{\sqrt{\frac{\sigma^2_{test}+\sigma^2_{bck}}{2}}}\right) \quad (1)$$

where μ and σ^2 are the mean and variance, respectively, of the grey scale distribution of the US image within the selected areas. The test area (*test*) was the most hyperechogenic marker (40 mm deep), while the background area (*bck*) was defined

as a circle adjacent to the test area at the same depth (**Errore. L'origine riferimento non è stata trovata.**b).

3) In-Vivo Test: Electrode-Skin Impedance and Noise: Maintaining low and balanced electrode-skin impedance across electrodes is crucial for detecting high-quality HD-sEMG, reducing movement artifacts [8], [40], [41], [42] and minimizing the effect of external sources of interference [40], [43], [44]. Therefore, it is paramount to characterize the electrode's impedance and its stability over time. ReGrid electrode-skin impedance magnitude was measured and compared to that of a standard grid of electrodes with a comparable electrode-skin contact area. To assess the temporal stability of the electrode-skin contact, impedance measurements for ReGrid were carried-out in two time points: immediately after electrode application and after the protocol for HD-sEMG quality assessment, described in the following sections. The time interval between the two measurements was approximately 60 minutes.

The impedance of the electrode-skin interface was measured for all consecutive electrode pairs in each column of the grid using a custom-made impedance-meter (LISiN, Politecnico di Torino, Italy [14], [45]). This device converts a sinusoidal voltage input into a proportional current signal (200 nA_{pp}) and measures the voltage drop between the electrodes tested. Both the sine wave, used to drive the current signal, and the voltage drop were sampled with a National Instrument data acquisition device (USB-6210, sampling frequency: 10 kHz, resolution of the A/D converter: 16 bits). The impedance magnitude was quantified as the ratio between the root-mean square amplitudes of the measured voltage drop and of the injected current, for a frequency sweep in the range 10 Hz–1000 Hz. The magnitude of the electrode-skin impedance at 50 Hz (power line frequency) was computed and normalized for the size of the electrode-skin interface.

Noise measurements were conducted ex-vivo on pigskin. This approach [45] was employed to simulate electrode-skin interface properties similar to those of human skin, in an experimental condition where no other physiological or electrical sources contribute to the detected noise. Using this experimental design, the only sources of the electrical potential are the noise from the electrode-skin interface and the electronic noise from the amplifier (measurable by short-circuiting the input electrodes). Since the electronics noise is uncorrelated with the electrode-skin interface noise [46], it can be removed through quadratic subtraction, isolating the electrode-skin interface from the electronic noise. The noise of the electrode-skin interface was measured though the MEACS HD-sEMG acquisition system (LISiN and ReC Bioengineering Laboratories S.r.l.–Turin, Italy) having the following characteristics: sampling frequency: 2048 Hz, amplification: 192 V/V, input range 10 mV_{pp}, 16 bits resolution, noise floor: 2.5 μV_{RTI} in the 10 Hz - 500 Hz frequency band [8].

4) In-Vivo Test: EMG Quality Assessment: The aims of the experimental protocol were the following: (i) to verify the quality of EMGs detected by ReGrid under experimental conditions similar to those commonly used in HD-sEMG studies and (ii) to assess the effects of placing the US probe over the electrodes on the characteristics of the detected EMG signal. To this end, HD-sEMG signals were recorded from the tibialis anterior (TA) muscle during isometric dorsiflexion of the foot. Signals were analyzed both at a global and single motor unit level.

The participant was positioned on the ergometer (Biodex System 4, Biodex Medical System, Shirley, USA) with a knee angle of approximately 120 degrees (where 180 degrees is full knee extension) and an ankle angle of 90 degrees. Before starting the experiment, the skin area over the right TA was shaved and then cleansed with abrasive paste (NuPrep, Weaver and Company, Aurora, USA). Two eight-by-four ReGrid (10 mm IED) were positioned on TA to obtain a grid of 64 (16×4) electrodes. The distal grid was placed with the first column of electrodes (column 1, Fig. 1b) 5 mm lateral to the anterior crest of the tibia bone and the first row of electrodes (row 1, Fig 1b) 1 cm proximal to the TA distal myotendinous junction. The anatomical landmarks were identified with ultrasound imaging (ArtUs, Telemed, Lithuania - equipped with a 12 MHz linear probe). The proximal grid was positioned so that the columns of electrodes in both grids were parallel to the TA's longitudinal axis (Fig. 1b). A pre-gelled reference electrode (Kendall, Cardinal Health, USA) was positioned on the lateral malleolus of the same leg. The grids were then connected to the MEACS acquisition systems (MEACS, ReC Bioengineering Laboratories, Turin, Italy) [8]. Force signals detected by Biodex were collected using a general-purpose acquisition system (GAM, ReC Bioengineering Laboratories, Turin, Italy) and synchronized with the HD-sEMG signals by means of a common digital signal wirelessly sent to both systems [47].

Monopolar HD-sEMG signals were recorded during an experimental protocol including six isometric contractions (5 s ramp-up phase, 20 s constant force phase at the target force). Force during the constant phase matched 10% and 20% of the maximum voluntary contraction (MVC), respectively for the first and last three contractions. For each group of contractions at the same target force (either 10% MVC or 20% MVC), the first two were acquired without the US probe over the grid (without US condition) while the third one was acquired with the US probe over the grid (with US condition). When placed over the grid, the US probe was positioned over the third row of the distal grid, transversally to the TA longitudinal axis.

a) Global EMG analysis: EMG signals detected under the two experimental conditions (with US and without US) were compared both in the time and frequency domains. The temporal analysis was focused on the morphology and spatiotemporal characteristics of the action potentials. Specifically, we examined the possibility of obtaining comparable estimates of conduction velocity (CV) in the distal muscle region. Indeed, any disturbances caused by the presence of the ultrasound probe are expected to induce common-mode artifacts, inflating CV estimates. CV was computed from a sequence of four consecutive single differential channels in the distal grid using the method described by Farina and colleagues [48], without including the muscle innervation zone. CV estimates were obtained for non-overlapping epochs of 500 ms during the 20 s steady phase of the 10% MVC

contraction, thus leading to forty estimates for each contraction. In addition to the CV analysis, the overall quality of the detected EMG signals was assessed by computing the signal-to-noise ratio (SNR) for each active channel and comparing SNR values between the two experimental conditions (*with US* and *without US*). The frequency domain analysis concerned the degree of power line interference and was motivated by the presence of a mains-powered US device whose probe is placed over the electrodes. This experimental setup is expected to increase the 50 Hz/60 Hz common mode voltage at the input of the electrode-amplifier system due to the parasitic coupling between the participant, the US device probe, and the power line mains and ground, thereby potentially increasing the amount of input-referred power line interference [11], [12], [49]. For each monopolar signal the signal power at mains frequency (a band of 4Hz centered around 50 Hz) was computed and normalized with respect to the total power of the signal (20 Hz - 400Hz). This variable was computed for the signals collected in the two experimental conditions (*with US* and *without US*) to assess whether the presence of the US probe increases the level of power line interference in the detected signals.

b) Single MU analysis: HD-sEMG decomposition was applied to the signals detected with ReGrid to demonstrate its suitability for single motor unit studies. We also aimed to show that the presence of the ultrasound probe on the electrodes does not affect the decomposition results. To this end, HD-sEMG signals were decomposed into their constituent motor unit action potential (MUAP) trains using a validated semi-automated algorithm [50], [51]. Spike trains were manually edited [52], and MUAPs were calculated using spike-triggered averaging with the identified firing instants as trigger source. For each contraction, the following variables were considered: (i) the number of identified motor units (MUs), (ii) the average Pulse-to-Noise Ratio (PNR) of the decomposed MUs, and (iii) the coefficient of variation (CoV) of the MU firing frequencies. Additionally, correlation coefficients (cc) [53] and normalized mean squared error (nMSE) [54] were used to match MUAPs identified in the first contraction (reference contraction - without US) with those identified in the following two test contractions at the same force level, one without (without US condition) and one with the US probe over the electrodes (with US condition). This approach allowed to evaluate whether the presence of the probe affected the ability to match MUAPs across different contractions. If the presence of the probe does not affect the signal quality, the decomposition results should be similar between the conditions with US and without US, moreover, the number of matched MUs between the reference and the test contraction should not depend on the presence of the probe.

C. Statistical Analysis

Shapiro-Wilk test was used to assess the normality of the collected variables' distributions. Parametric statistical tests were used in case of normal distribution, while non-parametric tests were adopted otherwise. Wilcoxon signed rank test was used to: (i) compare changes in magnitude of ReGrid electrode-skin impedances measured at the beginning ($|Z_{50}|_B$) and at the end ($|Z_{50}|_E$) of the experimental protocol and (ii) evaluate the effect of US probe over the electrodes on the signal-to-noise ratio (SNR) and on the relative power of the detected signals in the power line frequency band (48–52 Hz). Mann-Whitney test was used to compare the electrode-skin impedances and noise of ReGrid and conventional electrodes. A two-way ANOVA was used to analyze the effect of contraction level and the presence of the US probe over the electrodes on the MU decomposition results (PNR and ISI CoV) and on the descriptors of MU matches (cross correlation, nMSE). All statistical tests were performed in Matlab (version R2023a; The Math-Works, Natick, MA, USA). The threshold for statistical significance was set at $p < 0.05$ for all comparisons. Results are reported as median $\pm$ standard deviation.

III. Results

A. Bench Test: Conformability

Errore. L'origine riferimento non è stata trovata.a shows a standard grid and a ReGrid positioned on the 3D-printed semi-spherical solid with the intermediate radius (57 mm), among those tested. It is evident that state-of-the-art electrode grid displays several folds, particularly along its outer edges, indicating that it does not conform well to the curved surface of the semi-sphere and suggesting possible occurrence of bad contacts in the proximity of the folding. In contrast, ReGrid array adheres to the surface, showing no relevant deformations. These visual observations were supported by the quantification of missing electrical contacts between the grid electrodes and the conductive surface of the solid. For the standard grid, the number of missing contacts was 15, 9, and 2 for semi-spheres with radii of 41 mm, 57 mm, 78 mm respectively. In comparison, the ReGrid array exhibited no missing contacts for any of the tested radii.

B. Bench Test: Transparency to Ultrasound

Errore. L'origine riferimento non è stata trovata.b shows the two B-mode images detected from the phantom in the two experimental conditions: with and without the presence of ReGrid between the probe and the phantom. The quality of the two images was similar without evident artifacts due to the presence of ReGrid below the ultrasound probe. The similarity between the two images was confirmed by CNR that was 4.8 dB in the reference condition (without ReGrid) and 5.7 dB with ReGrid.

C. In-Vivo Tests: Electrode-Skin Impedance and Noise

Electrical characteristics of ReGrid and state-of-the-art electrode grid were comparable. No significant differences were observed both for the electrode-skin impedance magnitude at 50Hz and the input-referred electrode-skin noise (ReGrid vs conventional electrodes: 11.18 ± 2.89 k$\Omega\cdot$ cm^2 vs 10.42 ± 1.75 k$\Omega\cdot$ cm^2; 2.0 ± 1.1 μV_{RMS} vs 1.8 ± 1.0 μV_{RMS}). The comparison between the electrode-skin impedances measured for ReGrid electrodes at the beginning and at the

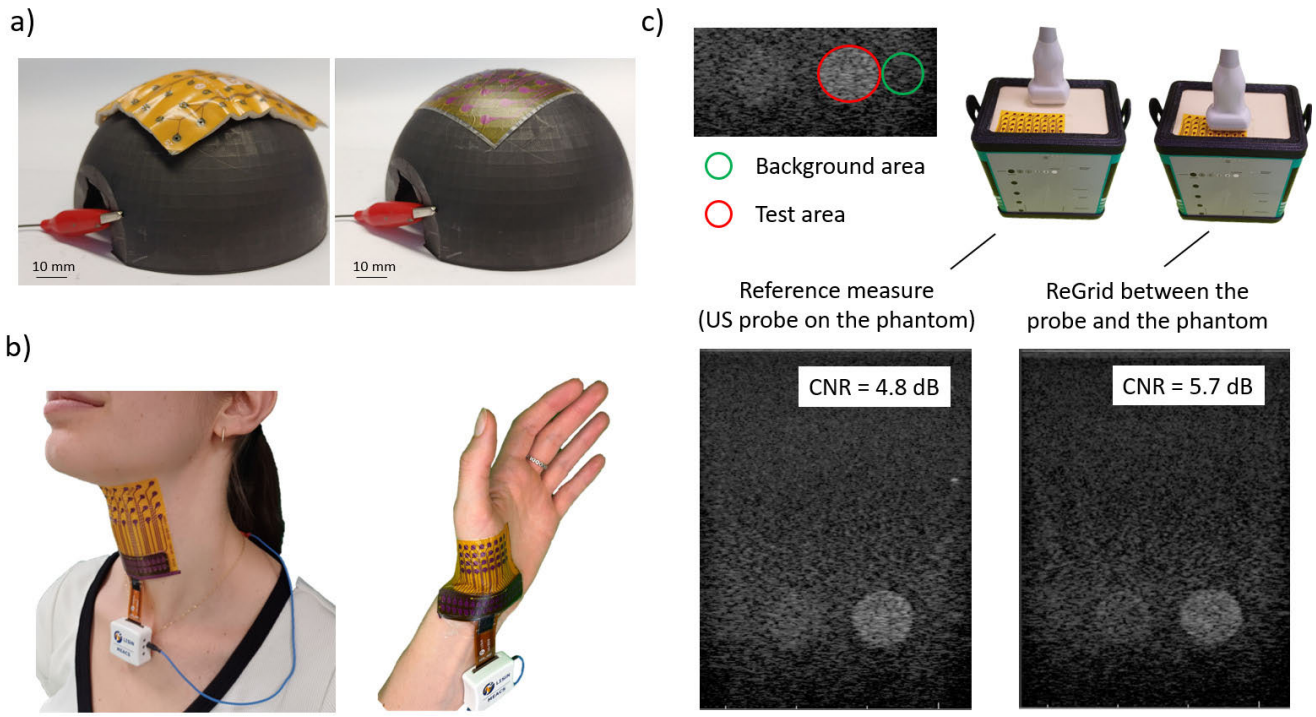

Fig. 2. Bench tests. a) A standard 64-channel HD-sEMG grid (left) and a 64-channel ReGrid patch (right), obtained by combining two 32-channel grids and positioned on a conductive semi-spherical solid (57 mm radius) to assess conformability. b) Examples of ReGrid positioning on infrahyoid muscles (grid with 10 mm IED) and on thenar eminence muscles (grid with 5 mm IED). c) Ultrasound transparency tests experimental setup and ultrasound images detected with and without the presence of ReGrid between the probe and the phantom.

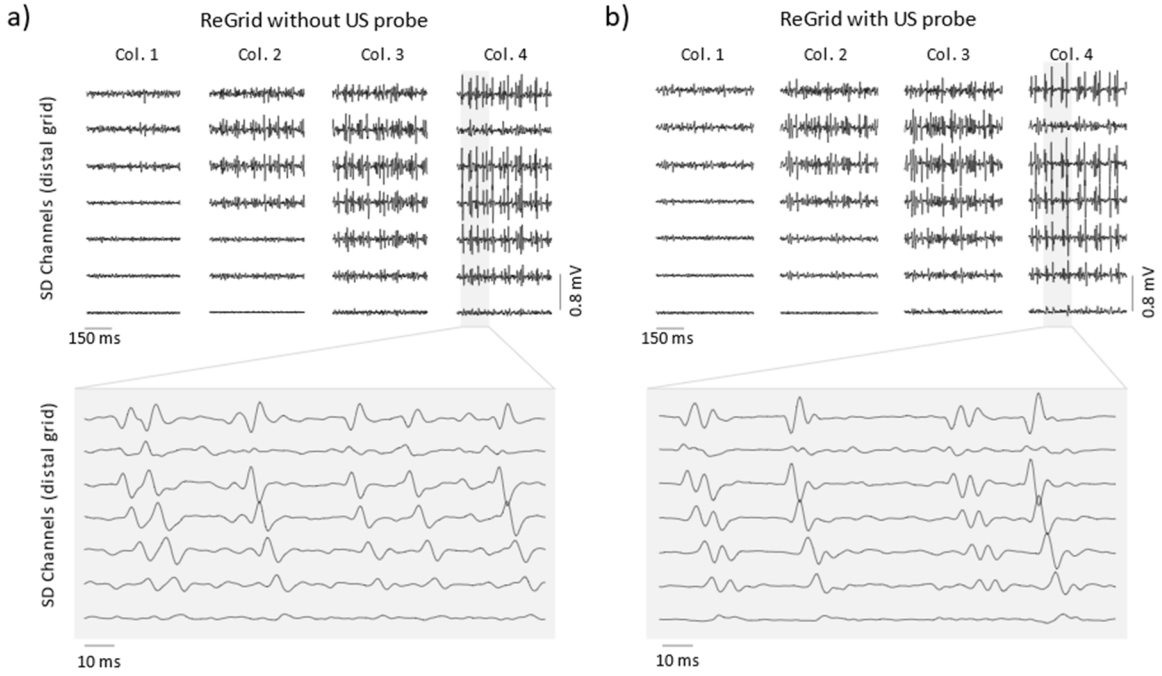

Fig. 3. Global EMG analysis. Two examples of raw HD-sEMG signals detected from the distal portion of the tibialis anterior during a 10%MVC isometric dorsiflexion with (a) and without (b) the US probe over the electrodes. The lower part of each panel shows a zoomed version of the signals of column 4 over a 150-ms epoch. Several propagating potentials and their innervation zones are clearly visible in both conditions.

end of the experimental protocol for HD-sEMG-US detection showed no significant differences (11.18 $\pm$ 2.89 kΩ·cm^2 vs 10.72 $\pm$ 1.33 kΩ·cm^2).

D. In-Vivo Test: EMG Quality Assessment

1) Global EMG Analysis: Fig. 3 shows the EMG signals recorded during a 10% MVC isometric dorsiflexion without

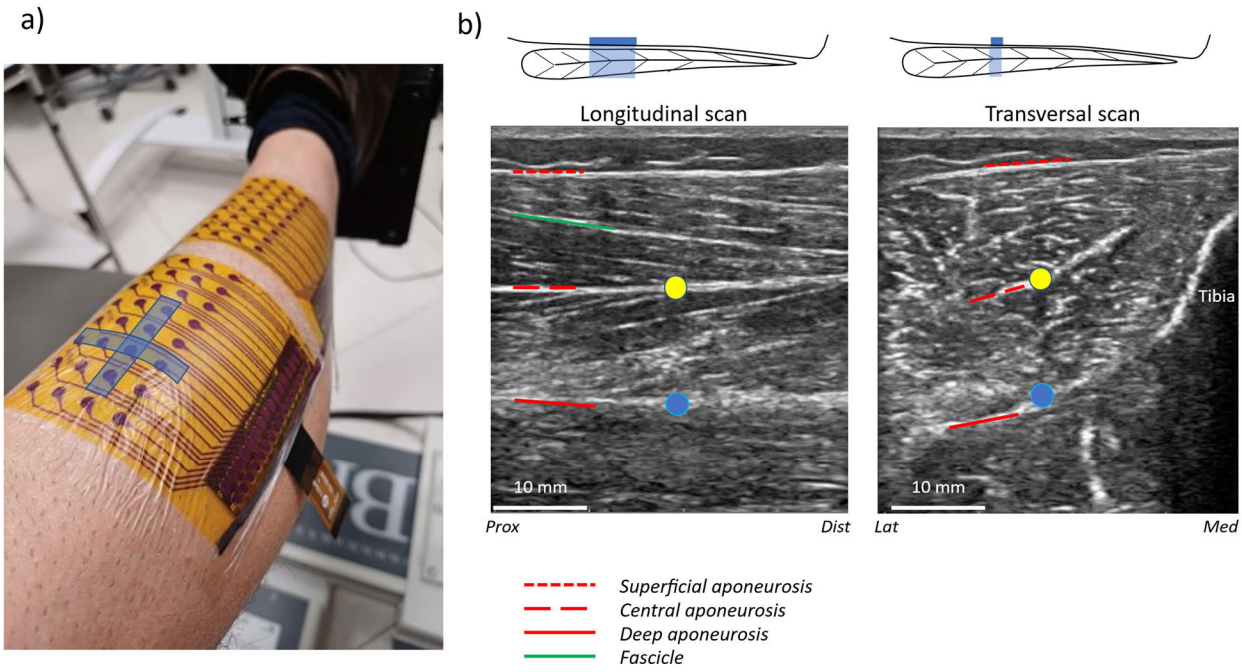

Fig. 4. Ultrasound images of the longitudinal and transverse sections of the tibialis anterior were obtained by placing the ultrasound probe on the surface of ReGrid. The position of the ultrasound probe is indicated with two blue rectangles on the left picture. Anatomical muscle structures, such as muscle fascicles and aponeuroses, are clearly visible in both ultrasound images.

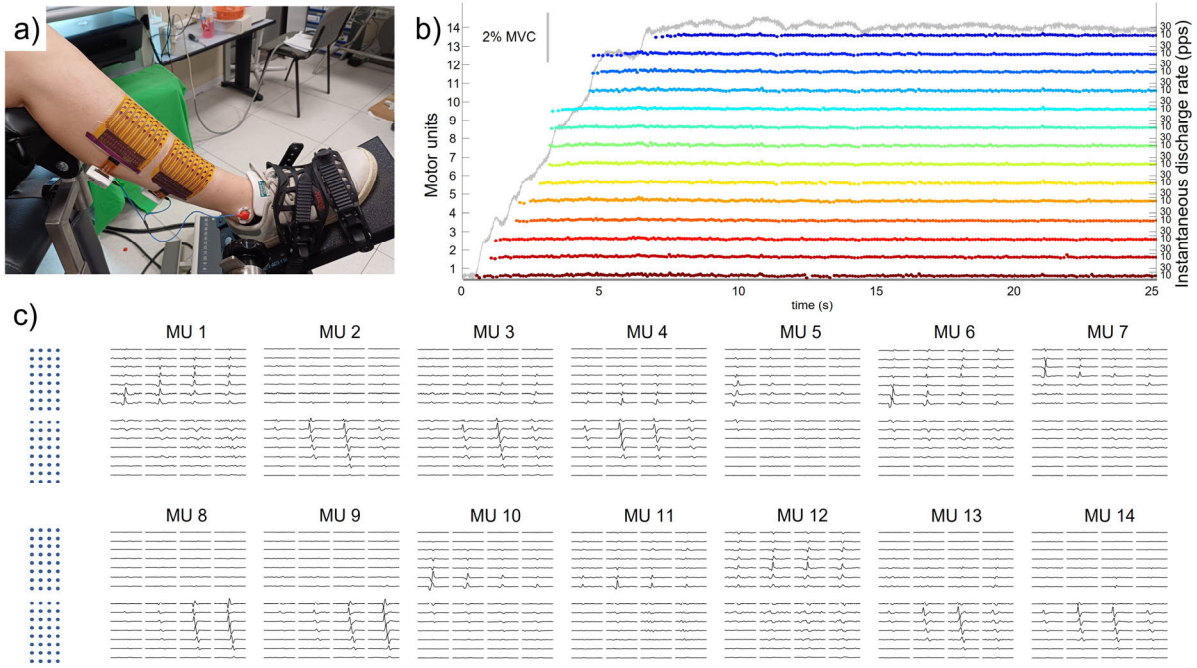

Fig. 5. Motor Unit (MU) identification from tibialis anterior during a 10% MVC isometric dorsiflexion. a) picture of the grid positioning. b) instantaneous firing rate of 14 MUs overlapped to the trapezoidal force profile. c) Single differential Motor Unit Action Potentials (MUAPs) obtained by the spike-triggered averaging based on MU firing instants of the raw HD-sEMG over a 50-ms window.

and with the US probe positioned over the grid. The presence of the probe over the electrode did not affect the estimates of average CV (with US vs without US: 3.50 $\pm$ 0.02 m/s vs 3.49 $\pm$ 0.02 m/s). The relative power in the 4-Hz frequency band centered on the power line frequency (50 Hz) did not change significantly in the two tested conditions (with US vs without US: 7.9 $\pm$ 1.9 % vs 7.0 $\pm$ 1.4 %, $p = 0.126$). Similarly, the SNR did not change significantly between the two conditions (with US vs without US, $p = 0.211$). Figure 4 shows two examples of B-mode US scans detected positioning

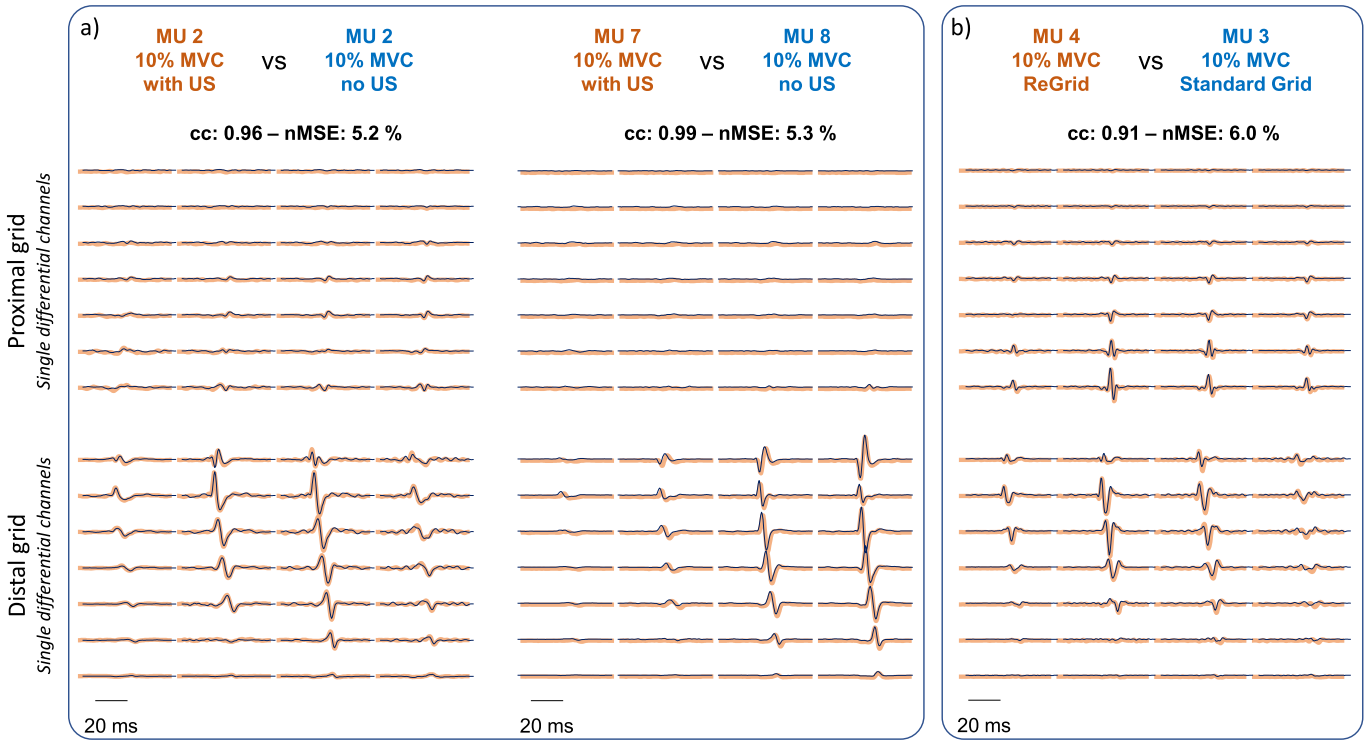

Fig. 6. a) Representative examples of matching between MUAPs identified during two different ankle dorsiflexions at 10% MVC performed with (orange trace) and without (blue trace) the joint acquisition of ultrasound images (i.e., with and without the ultrasound probe positioned on the electrode matrix). b) Comparison of the same MUAP identified across two 10% MVC contractions using ReGrid and a standard HD-sEMG grid (flexible polyimide circuit), positioned at the same anatomical location and with identical electrode configuration and size. For each pair of matched MUAPS the cross-correlation (cc) and the normalized mean squared error (nMSE) are reported.

TABLE I
DECOMPOSITION RESULTS AND EFFECT OF COMBINED HDSEMG-US ACQUISITION ON HDSEMG SIGNAL DECOMPOSITION

Contraction	Condition	# MUs	MU properties		MU matching		
			PNR (dB)	ISI CoV (%)	Matched MUs (w.r.t. Ref)	Cross-corr.	nMSE (%)
10% MVC (Ref)	Without US	15	32.4 ± 2.9	19.8 ± 1.1	n.a. (Ref)	n.a. (Ref)	n.a. (Ref)
10% MVC	Without US	14	33.7 ± 3.4	18.0 ± 1.7	10	0.973 ± 0.012	5.4 ± 2.3
10% MVC	With US	14	33.3 ± 4.2	18.4 ± 1.2	10	0.969 ± 0.011	6.2 ± 2.5
20% MVC (Ref)	Without US	13	31.7 ± 5.5	21.5 ± 3.0	n.a. (Ref)	n.a. (Ref)	n.a. (Ref)
20% MVC	Without US	12	30.1 ± 4.9	24.7 ± 8.4	8	0.984 ± 0.01	3.3 ± 1.8
20% MVC	With US	12	31.1 ± 5.6	20.6 ± 2.2	9	0.983 ± 0.01	3.5 ± 2.2

the US probe over ReGrid during the protocol for the EMG quality assessment. Anatomical structures such as aponeuroses and muscle fascicles are clearly visible.

2) Single Mu Analysis: Fig. 5 depicts a representative example of the decomposition results of a 10% MVC contraction. The characteristics of the decomposed MU pools for each contraction level and condition and the results of the MU matching across different contractions are reported in Table I. The presence of the US probe over the grid did not significantly affect the PNR ($p = 0.932$) and the ISI CoV ($p = 0.133$). As expected, ISI CoV was significantly affected by the contraction level, with larger CoV for 20% MVC contractions ($p < 0.001$). As regard to the MU matching, similar number of matched MUs with respect to the reference contraction could be found in the two test conditions: *with* and *without* US probe over the electrodes. The cross correlation and nMSE between matched MUs were not affected by the presence of the US probe ($p = 0.503$ and $p = 0.407$ respectively). A significant effect of the contraction level was observed for both cross correlation and nMSE ($p < 0.05$ and $p < 0.001$ respectively), with larger cross correlations and lower nMSE for the 20% MVC contraction. The examples in Fig. 6 illustrate the matching between MUAPs detected under the two experimental conditions, as well as the matching between MUAPs detected using ReGrid and a standard HD-sEMG grid (flexible polyimide circuit), both positioned at the same anatomical location and sharing identical electrode configuration and size.

IV. Discussion

A. Conformability and US Transparency

From a mechanical standpoint, ReGrid is a patch characterized by a thin profile and high conformability, making it minimally intrusive. These features enable recordings from uneven skin surfaces or regions that undergo significant shape changes during movement. In contrast, standard technology based on the use of bi-adhesive pads (1)-3 mm thickness) often encounters difficulties to conform to the underlying surfaces. The mechanical stresses at this interface can lead to a loss of electrode-skin contact resulting in power line interference and motion artifacts due to the high impedance (several hundreds of kilo-ohms) of the electrode-skin interface [40], [42], [44], [55]. The ReGrid reduced thickness, high conformability (implying the absence of air gaps between ReGrid and the skin), and the use of plastic materials determine its transparency to ultrasound. Previous studies have shown that the presence of air in the adhesive foam layer due to the relative rigidity of flexible PCB materials substantially hinder ultrasound transmission through electrode grids made with standard technology (cf. fig 1 in [22]). For this reason, electrode grids composed of materials with acoustic impedance similar to that of biological tissues, adhering uniformly to the skin, have been proposed [22]. In that implementation, the conductive tracks were embedded in a silicone material and were exposed only at the electrode sites in the grid. ReGrid represents a significant advancement in this technology, as the electrical pads and conductive tracks are printed directly on the material that forms the ultrasound-transparent patch. This eliminates the need for cavities in the supporting material, thereby reducing the thickness of the grid to that of the supporting patch itself.

In this work, we quantified the ultrasound transparency through an in-vitro test performed on a standard phantom. Results show that the image quality obtained with the grid positioned between the probe and the phantom is comparable to that obtained with the probe placed directly on the phantom. Ultrasound transparency is further shown in an in-vivo measurement of the tibialis anterior muscle (Fig 4b), where both longitudinal and transverse scans reveal the anatomical structures of the tibialis anterior without artifacts due to the presence of the grid between the probe and the skin. Notably, the ultrasound images presented in this study were obtained with the ultrasound probe positioned directly over the EMG electrodes, which also proved fully transparency to ultrasound. This is a particularly important feature for muscles demanding highly dense detection systems, such as those in the hand, where placing the US probe alongside the electrodes is not possible. Indeed, one possible approach that has been used to acquire HD-sEMG and ultrasound data from the same muscle region, is to introduce a gap (an US-window) between adjacent columns of electrodes in standard HD-sEMG grids to accommodate the ultrasound probe. While this is a feasible solution, it limits the minimum inter-electrode distance (electrode density) and requires protecting the electrodes from short-circuits mediated by the ultrasound gel. Additionally, this method does not allow for adjustments to the probe's position and orientation once the grid is in place. Finally, this solution does not allow to sweep the probe over the electrode grid, which is required for reconstructing a 3D volume of the muscle [56] and for panoramic/extended-field-of-view ultrasound imaging [57] Thanks to the full ultrasound transparency of ReGid, including the supporting layer and the electrodes, it is possible to acquire US image sequences while moving the probe over the muscle surface covered by the grid, as shown in the supplementary material.

B. Electrical Characterization and Signals Quality

ReGrid was found to be comparable to standard electrode grids in terms of both electrode-skin interface noise and impedance magnitude at 50Hz [14], [45], [58]. A key point of interest was the stability of the electrode-skin impedance over time. No significant variations in electrode-skin impedance magnitude at 50Hz were observed when comparing measurements taken at the beginning and end of the experimental protocol, which lasted about 60 minutes. It is worth noting that during the experimental protocol, water-based ultrasound gel was applied to the outer surface of the grid to perform joint HD-sEMG-US measurements. This gel could potentially penetrate between the grid and the skin generating low impedance paths between the electrodes or electrodes' detachment, thereby reducing the quality of the detected signals. The fact that the order of magnitude of the impedances remained stable from the start to the end of the measurements suggests that the electrode system is impermeable to external physical agents that could compromise signal quality.

The good quality of the electrode-skin contact is reflected in performance in terms of power line interference rejection properties of the electrode-amplifier system. It is well known that the degree of power line interference affecting biopotentials depends on the common-mode voltage at the input of the electrode-amplifier system [10], [11], [12]. This voltage is primarily due to parasitic capacitive coupling between the participant, the power line source, and the ground, as well as coupling between the front-end reference and the power line ground [11], [59]. This common-mode voltage can be converted into a differential signal at the amplifier's input due to the so-called voltage divider effect [10], [12], [60]. Having low and homogeneous impedance across the electrodes contributes to minimize this effect. It is also important to note that in the case of concurrent HD-sEMG and ultrasound measurements, the presence of the ultrasound probe (connected to a mains-powered device) in contact with the electrode grid could strengthen the capacitive coupling of the electrodes with the power line mains, consequently increasing the 50Hz/60Hz common-mode voltage at the input of the electrodes-amplifier system. Our experimental measurements showed that this condition does not lead to a significant increase in power within a 4-Hz frequency band centered to the power line frequency (50 Hz). This result is likely due to two main factors: i) the relatively low 50-Hz electrode-skin impedance magnitude with respect to the amplifier input impedance, limiting the voltage divider effect; ii) the use of a miniaturized and ground-floating wireless acquisition system

[8], [12], decoupling front-end electronics form the power line mains and ground.

C. Global HD-sEMG Analysis

The analysis of HD-sEMG signals detected using ReGrid allowed for the extraction of physiologically relevant variables both at the global and individual motor unit levels. Given the extensive literature on HD-sEMG studies using standard grids, here we focused on comparing performance of ReGrid with and without the probe over the grid, using literature values as reference for comparison with standard grids. This analysis was performed because, despite the good rejection of power line interference, the presence of the probe could potentially introduce artifacts or other disturbances that might limit the extraction of relevant information from HD-sEMG signals. For the global features extracted from experimental signals, we focused on CV estimation, a key physiological variable for characterizing the propagation of action potentials along the muscle fiber membrane [61]. The estimation of CV from sEMG signals relies on calculating the time delay between signals recorded by electrodes placed along the course of the muscle fibers [62]. Calculating CV is therefore particularly sensitive to artifacts or disturbances that appear simultaneously across multiple electrodes, as these can bias the time delay estimation and consequently lead to overestimations. Our results indicate that CV estimates are not affected by the presence of the ultrasound probe over the electrodes, suggesting that signals quality remains unchanged even under joint HD-sEMG-US measurement conditions.

D. Single MU Analysis

The analysis at the single motor unit level demonstrated that the decomposition of signals detected by ReGrid yields results comparable to those reported in the literature, in terms of both the number and characteristics of the identified motor units. Additionally, the presence of the ultrasound probe on the electrode grid did not affect the decomposition output. The analysis of matched single motor units (MU tracking) was specifically designed to test the effect of the combined EMG-US measures on the firing properties of the identified motor units and on the shape of the identified action potentials. We conducted motor unit tracking across consecutive contractions without changing the position of the participant or the grid, to minimize potential confounding factors that could alter the action potential shape [53]. This setup was purposely chosen as it provides favorable conditions for motor unit tracking, allowing us to isolate possible effects of the presence of the ultrasound probe on the grid. For both force levels, when compared to the reference contraction, neither the number of matches nor the values of the considered metrics were significantly affected by the presence of the ultrasound probe. In line with the results from the global signal analysis, this finding complements the previously shown analyses of noise, impedance, and power line interference, demonstrating that the proposed electrode grid performs similarly to standard electrodes and enables the extraction of physiologically relevant variables even during combined measurements with ultrasound.

From a broader perspective, ReGrid grid enables a range of new experimental paradigms for the study of neuromuscular function. By allowing the concurrent acquisition of high-quality HD-sEMG signals and ultrasound images from the same muscle region, this technology enables the characterization of the electromechanical properties of muscle contraction, including the relationship between neural drive, tissue motion, and architectural changes. In addition, the technology presented in this study opens the way to three-dimensional imaging of muscle, either by moving the US probe over the electrodes or by using 2D matrix array transducers, facilitating volumetric reconstructions of muscle morphology. Integrated recordings may help linking changes in muscle architecture to changes in EMG features at both the global level (e.g. amplitude distribution) and the single motor unit level (e.g. MUAP waveform). This may provide useful information to enhance the modelling of the relationship between muscle architecture and MUAP shape, with potential benefits for the improvement of HD-sEMG decomposition algorithms in dynamic contractions. Finally, the waterproof nature of the proposed grid may enable EMG investigations in aquatic environments, expanding opportunities for studying muscle function under altered loading conditions. From a technological perspective, ReGrid represents a new generation of electrode-grid technology compared to conventional PCB-based solutions with bi-adhesive foams, providing high conformability complex anatomical surfaces and robust interfacing with signal conditioning and acquisition systems. Although the experimental validation presented in this study was performed using a grid configuration with a 10 mm inter-electrode distance, the proposed technology is not limited to this spacing and number of electrodes. ReGrid can be scaled to different electrode configurations, including higher-density layouts (i.e. 5 mm IED, Fig 2.b), depending on the requirements of the application.

V. Conclusion

In this work we described the design, development and characterization of an innovative fully echo-transparent HD-sEMG electrode patch. The developed detection system represents an advancement of the state-of-the-art technology for the concurrent acquisition of HD-sEMG signals and US images through highly conformable grids of electrodes. The design methodology, bench, and in-vivo characterization demonstrated that the developed detection system can be considered an enabling technoly for the development of new applications requiring high conformability of the electrodes grids, waterproofness or the simultaneous acquisition of high quality HD-sEMG signals and US images. Although presented in the context of surface EMG detection, the proposed electrode design is extendable to other applications involving the acquisition of surface biopotentials, further broadening the potential impact of this technology.

Conflicts of Interest

The authors are involved in the activities of ReC Bioengineering Laboratories S.r.l., Torino, Italy; and the academic spin-off of the Laboratory for Engineering of the Neuromuscular System, Politecnico di Torino, Torino, which commercializes medical devices for the acquisition of HD-sEMG signals. The authors hold the Italian patent application n. 102023000026523 and the PCT application n. PCT/IB2024/062483 related to the technology described in this article.

References

[1] D. Farina and R. M. Enoka, "Evolution of surface electromyography: From muscle electrophysiology towards neural recording and interfacing," *J. Electromyogr. Kinesiol.*, vol. 71, Aug. 2023, Art. no. 102796, doi: 10.1016/j.jelekin.2023.102796.

[2] M. M. Gomes, S. T. Jenz, J. A. Beauchamp, F. Negro, C. J. Heckman, and G. E. P. Pearcey, "Voluntary co-contraction of ankle muscles alters motor unit discharge characteristics and reduces estimates of persistent inward currents," *J. Physiol.*, vol. 602, no. 17, pp. 4237–4250, Sep. 2024, doi: 10.1113/jp286539.

[3] G. L. Cerone, R. Nicola, M. Caruso, R. Rossanigo, A. Cereatti, and T. M. Vieira, "Running speed changes the distribution of excitation within the biceps femoris muscle in 80 m sprints," *Scandin. J. Med. Sci. Sports*, vol. 33, no. 7, pp. 1104–1115, Jul. 2023, doi: 10.1111/sms.14341.

[4] F. V. dos Anjos, M. Ghislieri, G. L. Cerone, T. P. Pinto, and M. Gazzoni, "Changes in the distribution of muscle activity when using a passive trunk exoskeleton depend on the type of working task: A high-density surface EMG study," *J. Biomechanics*, vol. 130, Jan. 2022, Art. no. 110846, doi: 10.1016/j.jbiomech.2021.110846.

[5] R. Merletti, M. Aventaggiato, A. Botter, A. Holobar, H. Marateb, and T. M. M. Vieira, "Advances in surface EMG: Recent progress in detection and processing techniques," *Crit. Rev. Biomed. Eng.*, vol. 38, no. 4, pp. 305–345, 2010, doi: 10.1615/critrevbiomedeng.v38.i4.10.

[6] T. M. Vieira and A. Botter, "The accurate assessment of muscle excitation requires the detection of multiple surface electromyograms," *Exercise Sport Sci. Rev.*, vol. 49, no. 1, pp. 23–34, Jan. 2021, doi: 10.1249/jes.0000000000000240.

[7] D. Farina, R. Merletti, and R. M. Enoka, "The extraction of neural strategies from the surface EMG: 2004–2024," *J. Appl. Physiol.*, vol. 138, no. 1, pp. 121–135, Jan. 2025, doi: 10.1152/japplphysiol.00453.2024.

[8] G. L. Cerone, A. Botter, and M. Gazzoni, "A modular, smart, and wearable system for high density sEMG detection," *IEEE Trans. Biomed. Eng.*, vol. 66, no. 12, pp. 3371–3380, Dec. 2019, doi: 10.1109/TBME.2019.2904398.

[9] D. P. Dobrev and T. D. Neycheva, "High-quality biopotential acquisition without a reference electrode: Power-line interference reduction by adaptive impedance balancing in a mixed analog–digital design," *Med. Biol. Eng. Comput.*, vol. 60, no. 6, pp. 1801–1814, Jun. 2022, doi: 10.1007/s11517-022-02586-0.

[10] J. C. Huhta and J. G. Webster, "60-Hz interference in electrocardiography," *IEEE Trans. Biomed. Eng.*, vol. BME-20, no. 2, pp. 91–101, Mar. 1973, doi: 10.1109/TBME.1973.324169.

[11] A. C. Metting van Rijn, A. Peper, and C. A. Grimbergen, "High-quality recording of bioelectric events: Part 1 interference reduction, theory and practice," *Med. Biol. Eng. Comput.*, vol. 28, no. 5, pp. 389–397, Sep. 1990, doi: 10.1007/bf02441961.

[12] R. Merletti and G. L. Cerone, "Tutorial. Surface EMG detection, conditioning and pre-processing: Best practices," *J. Electromyogr. Kinesiol.*, vol. 54, Oct. 2020, Art. no. 102440, doi: 10.1016/j.jelekin.2020.102440.

[13] A. Spanu, A. Botter, A. Zedda, G. L. Cerone, A. Bonfiglio, and D. Pani, "Dynamic surface electromyography using stretchable screen-printed textile electrodes," *IEEE Trans. Neural Syst. Rehabil. Eng.*, vol. 29, pp. 1661–1668, 2021, doi: 10.1109/TNSRE.2021.3104972.

[14] G. L. Cerone, A. Botter, T. Vieira, and M. Gazzoni, "Design and characterization of a textile electrode system for the detection of high-density sEMG," *IEEE Trans. Neural Syst. Rehabil. Eng.*, vol. 29, pp. 1110–1119, 2021, doi: 10.1109/TNSRE.2021.3086860.

[15] G. Rolandino, M. Gagliardi, T. Martins, G. L. Cerone, B. Andrews, and J. J. FitzGerald, "Developing RPC-Net: Leveraging high-density electromyography and machine learning for improved hand position estimation," *IEEE Trans. Biomed. Eng.*, vol. 71, no. 5, pp. 1617–1627, May 2024, doi: 10.1109/TBME.2023.3346192.

[16] E. Martinez-Valdes et al., "Modulations in motor unit discharge are related to changes in fascicle length during isometric contractions," *J. Appl. Physiol.*, vol. 133, no. 5, pp. 1136–1148, Nov. 2022, doi: 10.1152/japplphysiol.00758.2021.

[17] A. Botter, T. Vieira, M. Carbonaro, G. L. Cerone, and E. F. Hodson-Tole, "Electrodes' configuration influences the agreement between surface EMG and B-mode ultrasound detection of motor unit fasciculation," *IEEE Access*, vol. 9, pp. 98110–98120, 2021, doi: 10.1109/ACCESS.2021.3094665.

[18] M. Carbonaro, K. M. Meiburger, S. Seoni, E. F. Hodson-Tole, T. Vieira, and A. Botter, "Physical and electrophysiological motor unit characteristics are revealed with simultaneous high-density electromyography and ultrafast ultrasound imaging," *Sci. Rep.*, vol. 12, no. 1, pp. 1–14, May 2022, doi: 10.1038/s41598-022-12999-4.

[19] R. Rohlén, M. Carbonaro, G. L. Cerone, K. M. Meiburger, A. Botter, and C. Grönlund, "Spatially repeatable components from ultrafast ultrasound are associated with motor unit activity in human isometric contractions *," *J. Neural Eng.*, vol. 20, no. 4, Aug. 2023, Art. no. 046016, doi: 10.1088/1741-2552/ace6fc.

[20] E. Lubel, B. Grandi Sgambato, D. Y. Barsakcioglu, J. Ibáñez, M.-X. Tang, and D. Farina, "Kinematics of individual muscle units in natural contractions measured in vivo using ultrafast ultrasound," *J. Neural Eng.*, vol. 19, no. 5, Oct. 2022, Art. no. 056005, doi: 10.1088/1741-2552/ac8c6c.

[21] T. M. Vieira, M. C. Bisi, R. Stagni, and A. Botter, "Changes in tibialis anterior architecture affect the amplitude of surface electromyograms," *J. NeuroEng. Rehabil.*, vol. 14, no. 1, p. 81, Aug. 2017, doi: 10.1186/s12984-017-0291-5.

[22] A. Botter, T. M. M. Vieira, I. D. Loram, R. Merletti, and E. F. Hodson-Tole, "A novel system of electrodes transparent to ultrasound for simultaneous detection of myoelectric activity and B-mode ultrasound images of skeletal muscles," *J. Appl. Physiol.*, vol. 115, no. 8, pp. 1203–1214, Oct. 2013, doi: 10.1152/japplphysiol.00090.2013.

[23] R. J. Varghese, M. Pizzi, A. Kundu, A. Grison, E. Burdet, and D. Farina, "Design, fabrication and evaluation of a stretchable high-density electromyography array," *Sensors*, vol. 24, no. 6, p. 1810, Mar. 2024, doi: 10.3390/s24061810.

[24] G. Rolandino, C. Zangrandi, T. Vieira, G. L. Cerone, B. Andrews, and J. J. FitzGerald, "HDE-array: Development and validation of a new dry electrode array design to acquire HD-sEMG for hand position estimation," *IEEE Trans. Neural Syst. Rehabil. Eng.*, vol. 32, pp. 4004–4013, 2024, doi: 10.1109/TNSRE.2024.3490796.

[25] A. Botter, T. Vieira, C. Busso, F. Vitali, M. Gazzoni, and G. L. Cerone, "Design and test of an intraoral electrode grid for tongue high-density electromyography," *IEEE Trans. Neural Syst. Rehabil. Eng.*, vol. 32, pp. 2805–2814, 2024, doi: 10.1109/TNSRE.2024.3434360.

[26] Y. Zhao, C. Chen, B. Lu, X. Zhu, and G. Gu, "All 3D-printed soft high-density surface electromyography electrode arrays for accurate muscle activation mapping and decomposition," *Adv. Funct. Mater.*, vol. 34, no. 14, pp. 1–14, Apr. 2024, doi: 10.1002/adfm.202312480.

[27] P. F. Shahandashti, H. Pourkheyrollah, A. Jahanshahi, and H. Ghafoorifard, "Highly conformable stretchable dry electrodes based on inexpensive flex substrate for long-term biopotential (EMG/ECG) monitoring," *Sens. Actuators A, Phys.*, vol. 295, pp. 678–686, Aug. 2019, doi: 10.1016/j.sna.2019.06.041.

[28] N. Driscoll et al., "MXene-infused bioelectronic interfaces for multiscale electrophysiology and stimulation," *Sci. Transl. Med.*, vol. 13, no. 612, pp. 1–28, Sep. 2021, doi: 10.1126/scitranslmed.abf8629.

[29] B. B. Murphy et al., "A gel-free $Ti_3C_2T_x$-based electrode array for high-density, high-resolution surface electromyography," *Adv. Mater. Technol.*, vol. 5, no. 8, Aug. 2020, doi: 10.1002/admt.202000325.

[30] A. Spanu et al., "Spray-coated, magnetically connectable free-standing epidermal electrodes for high quality biopotential recordings," *Adv. Eng. Mater.*, vol. 26, no. 11, pp. 1–10, Jun. 2024, doi: 10.1002/adem.202302195.

[31] M. R. Carneiro, C. Majidi, and M. Tavakoli, "Multi-electrode printed bioelectronic patches for long-term electrophysiological monitoring," *Adv. Funct. Mater.*, vol. 32, no. 43, pp. 1–15, Oct. 2022, doi: 10.1002/adfm.202205956.

[32] S. Velasco-Bosom et al., "Conducting polymer-ionic liquid electrode arrays for high-density surface electromyography," *Adv. Healthcare Mater.*, vol. 10, no. 17, pp. 1–6, Sep. 2021, doi: 10.1002/adhm.202100374.

[33] F. Ershad et al., "Customizable, reconfigurable, and anatomically coordinated large-area, high-density electromyography from drawn-on-skin electrode arrays," *PNAS Nexus*, vol. 2, no. 1, pp. 1–14, Jan. 2023, doi: 10.1093/pnasnexus/pgac291.

[34] S. Chandra et al., "Performance evaluation of a wearable tattoo electrode suitable for high-resolution surface electromyogram recording," *IEEE Trans. Biomed. Eng.*, vol. 68, no. 4, pp. 1389–1398, Apr. 2021, doi: 10.1109/TBME.2020.3032354.

[35] A. Botter, M. Beltrandi, G. L. Cerone, M. Gazzoni, and T. M. M. Vieira, "Development and testing of acoustically-matched hydrogel-based electrodes for simultaneous EMG-ultrasound detection," *Med. Eng. Phys.*, vol. 64, no. 1, pp. 74–79, Feb. 2019, doi: 10.1016/j.medengphy.2018.12.002.

[36] C. Leitner et al., "UStEMG: An ultrasound transparent tattoo-based sEMG system for unobtrusive parallel acquisitions of muscle electro-mechanics," Tech. Rep., 2021. [Online]. Available: https://ieeexplore.ieee.org/abstract/document/9630034

[37] L. Li et al., "Synchronized ultrasonography and electromyography signals detection enabled by nanocellulose based ultrasound transparent electrodes," *Carbohydrate Polym.*, vol. 347, Jan. 2025, Art. no. 122641, doi: 10.1016/j.carbpol.2024.122641.

[38] D. Zhang et al., "Stretchable and durable HD-sEMG electrodes for accurate recognition of swallowing activities on complex epidermal surfaces," *Microsyst. Nanoeng.*, vol. 9, no. 1, pp. 7077–7082, Sep. 2023, doi: 10.1038/s41378-023-00591-3.

[39] D. Queen, J. H. Evans, J. D. S. Gaylor, J. M. Courtney, and W. H. Reid, "An in vitro assessment of wound dressing conformability," *Biomaterials*, vol. 8, no. 5, pp. 372–376, 1987, doi: 10.1016/0142-9612(87)90008-1.

[40] A. Giangrande, A. Botter, H. Piitulainen, and G. L. Cerone, "Motion artifacts in dynamic EEG recordings: Experimental observations, electrical modelling, and design considerations," *Sensors*, vol. 24, no. 19, p. 6363, Sep. 2024, doi: 10.3390/s24196363.

[41] G. L. Cerone and M. Gazzoni, "A wireless, minaturized multi-channel sEMG acquisition system for use in dynamic tasks," in *Proc. IEEE Biomed. Circuits Syst. Conf. (BioCAS)*, Oct. 2017, pp. 1–4, doi: 10.1109/BIOCAS.2017.8325129.

[42] J. G. Webster, "Reducing motion artifacts and interference in biopotential recording," *IEEE Trans. Biomed. Eng.*, vol. BME-31, no. 12, pp. 823–826, Dec. 1984, doi: 10.1109/TBME.1984.325244.

[43] H. D. Talhouet and J. G. Webster, "The origin of skin-stretch-caused motion artifacts under electrodes," *Physiolog. Meas.*, vol. 17, no. 2, pp. 81–93, May 1996, doi: 10.1088/0967-3334/17/2/003.

[44] A. B. Simakov and J. G. Webster, "Motion artifact from electrodes and cables," *Iranian J. Elect. Comput. Eng.*, vol. 9, no. 2, pp. 139–143, 2010.

[45] G. Piervirgili, F. Petracca, and R. Merletti, "A new method to assess skin treatments for lowering the impedance and noise of individual gelled Ag–AgCl electrodes," *Physiolog. Meas.*, vol. 35, no. 10, pp. 2101–2118, Oct. 2014, doi: 10.1088/0967-3334/35/10/2101.

[46] E. Huigen, A. Peper, and C. A. Grimbergen, "Investigation into the origin of the noise of surface electrodes," *Med. Biol. Eng. Comput.*, vol. 40, no. 3, pp. 332–338, May 2002, doi: 10.1007/bf02344216.

[47] G. L. Cerone, A. Giangrande, M. Ghislieri, M. Gazzoni, H. Piitulainen, and A. Botter, "Design and validation of a wireless body sensor network for integrated EEG and HD-sEMG acquisitions," *IEEE Trans. Neural Syst. Rehabil. Eng.*, vol. 30, pp. 61–71, 2022, doi: 10.1109/TNSRE.2022.3140220.

[48] D. Farina, W. Muhammad, E. Fortunato, O. Meste, R. Merletti, and H. Rix, "Estimation of single motor unit conduction velocity from surface electromyogram signals detected with linear electrode arrays," *Med. Biol. Eng. Comput.*, vol. 39, no. 2, pp. 225–236, Mar. 2001, doi: 10.1007/bf02344807.

[49] M. Haberman, A. Cassino, and E. Spinelli, "Estimation of stray coupling capacitances in biopotential measurements," *Med. Biol. Eng. Comput.*, vol. 49, no. 9, pp. 1067–1071, Sep. 2011, doi: 10.1007/s11517-011-0811-6.

[50] A. Holobar and D. Zazula, "Multichannel blind source separation using convolution kernel compensation," *IEEE Trans. Signal Process.*, vol. 55, no. 9, pp. 4487–4496, Sep. 2007, doi: 10.1109/TSP.2007.896108.

[51] A. Holobar, M. A. Minetto, A. Botter, F. Negro, and D. Farina, "Experimental analysis of accuracy in the identification of motor unit spike trains from high-density surface EMG," *IEEE Trans. Neural Syst. Rehabil. Eng.*, vol. 18, no. 3, pp. 221–229, Jun. 2010, doi: 10.1109/TNSRE.2010.2041593.

[52] A. Del Vecchio, A. Holobar, D. Falla, F. Felici, R. M. Enoka, and D. Farina, "Tutorial: Analysis of motor unit discharge characteristics from high-density surface EMG signals," *J. Electromyogr. Kinesiol.*, vol. 53, Aug. 2020, Art. no. 102426, doi: 10.1016/j.jelekin.2020.102426.

[53] E. Martinez-Valdes, F. Negro, C. M. Laine, D. Falla, F. Mayer, and D. Farina, "Tracking motor units longitudinally across experimental sessions with high-density surface electromyography," *J. Physiol.*, vol. 595, no. 5, pp. 1479–1496, Mar. 2017, doi: 10.1113/jp273662.

[54] D. Farina, F. Negro, M. Gazzoni, and R. M. Enoka, "Detecting the unique representation of motor-unit action potentials in the surface electromyogram," *J. Neurophysiol.*, vol. 100, no. 3, pp. 1223–1233, Sep. 2008, doi: 10.1152/jn.90219.2008.

[55] H. Tam and J. G. Webster, "Minimizing electrode motion artifact by skin abrasion," *IEEE Trans. Biomed. Eng.*, vol. BME-24, no. 2, pp. 134–139, Mar. 1977, doi: 10.1109/TBME.1977.326117.

[56] L. Barber, R. Barrett, and G. Lichtwark, "Validation of a freehand 3D ultrasound system for morphological measures of the medial gastrocnemius muscle," *J. Biomechanics*, vol. 42, no. 9, pp. 1313–1319, Jun. 2009, doi: 10.1016/j.jbiomech.2009.03.005.

[57] M. V. Franchi, D. P. Fitze, J. Hanimann, F. Sarto, and J. Spörri, "Panoramic ultrasound vs. MRI for the assessment of hamstrings cross-sectional area and volume in a large athletic cohort," *Sci. Rep.*, vol. 10, no. 1, pp. 1–10, Aug. 2020, doi: 10.1038/s41598-020-71123-6.

[58] P. Cattarello and R. Merletti, "Characterization of dry and wet electrode-skin interfaces on different skin treatments for HDsEMG," in *Proc. IEEE Int. Symp. Med. Meas. Appl. (MeMeA)*, May 2016, pp. 1–6, doi: 10.1109/MEMEA.2016.7533808.

[59] M. F. Chimene and R. Pallas-Areny, "A comprehensive model for power line interference in biopotential measurements," *IEEE Trans. Instrum. Meas.*, vol. 49, no. 3, pp. 535–540, Jun. 2000, doi: 10.1109/19.850390.

[60] R. Merletti, A. Botter, A. Troiano, E. Merlo, and M. A. Minetto, "Technology and instrumentation for detection and conditioning of the surface electromyographic signal: State of the art," *Clin. Biomechanics*, vol. 24, no. 2, pp. 122–134, Feb. 2009, doi: 10.1016/j.clinbiomech.2008.08.006.

[61] S. Andreassen and L. Arendt-Nielsen, "Muscle fibre conduction velocity in motor units of the human anterior tibial muscle: A new size principle parameter," *J. Physiol.*, vol. 391, no. 1, pp. 561–571, Oct. 1987, doi: 10.1113/jphysiol.1987.sp016756.

[62] D. Farina and R. Merletti, "Methods for estimating muscle fibre conduction velocity from surface electromyographic signals," *Med. Biol. Eng. Comput.*, vol. 42, no. 4, pp. 432–445, Jul. 2004, doi: 10.1007/bf02350984.